The ripple-curry amplifier in photonic applications

Marian Gilewski

Faculty of Electrical Engineering, Bialystok University of Technology, Wiejska 45A, 15-351 Bialystok

Received December 21, 2022; accepted December 27, 2022; published December 31, 2022

Abstract—This paper discusses the new design of a amplifier for the miniature MEMS-type spectrometer. The application problem of the new amplifier was the correct conditioning of the sensor's photoelectric pulses. The processed signal was a sequence of pulses that had variable both frequency and amplitude value. Thus, such a broadband amplifier should have the functionality of automatic gain control. This paper describes the concept of the new circuit, develops its detailed application, and then performs validation tests. Measurement results of the new circuit are discussed in the final section of the paper.

Optical radiation measurements have specific features in comparison with general metrology. The main distinguishing feature is the large range of input signal variation. Therefore, the photo-detector signal (Fig. 1) must be amplified by an adjustable gain amplifier [1–3]. This is necessary because the input signal of the analog-to-digital converter should have a sufficiently large value. The signal processing path, shown in Fig. 1, is often used to measure basic light parameters. Due to measurement quality, the most important component of this chain is the variable photodetector-amplifier.

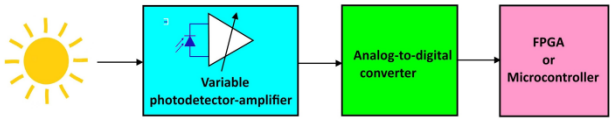

Fig. 1. A typical light measurement path.

Nowadays, precision amplifiers for photoelectric signals are available, some of which include an internal photodetector too [4]. These single-channel amplifiers (Fig. 2), by changing their measurement ranges, can handle optical signals that change their values over a very wide range. However, despite the advanced technology, such amplifiers have one major disadvantage, the dependence of the amplifier's frequency bandwidth on the

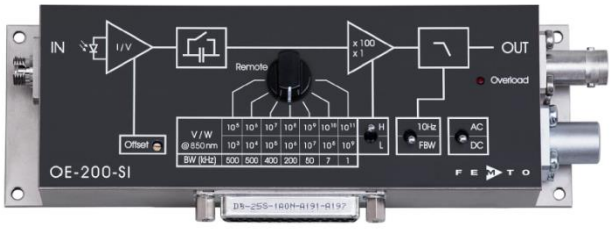

Fig. 2. View of the commercial photodetector with variable gain [4].

gain value. This relationship is shown in Table 1. It shows that for the gain value of 10^4 V/W, the discussed amplifier can handle input signals in frequencies up to 500 kHz without distortion. On the other hand, if the gain is as high as 10^8 V/W, the highest frequency of the input signal should be 7 kHz. A high-quality amplifier should hold the same frequency bandwidth for all gain values.

Tab. 1. Selected parameters of the variable gain photoreceiver [4].

Conversion Gain [V/W]	10^3	10^4	10^5	10^6	10^7	10^8	10^9
Bandwidth (–3 dB) [kHz]	500	500	400	200	50	7	1.1
Rise Time (10%–90%) [µs]	0.7	0.7	0.9	1.8	7.0	50	300

Like frequency band stability, pulse rise time is the important parameter in some applications. These two parameters are correlated, with rise time being more important for light sensors where the electrical output signal is pulsed. Pulse modulation of the output signal is necessary if one output signal transmits more information. This occurs, for example, in integrated micro-spectrometers. Such miniature MEMS spectrometer solutions are becoming more common and the technology is being further developed [5–11]. An example of this category of radiation transducers can be the C12666MA [12] chip, which selected time characteristics are shown in Fig. 3. In this figure, the yellow waveform represents

Fig. 3. View of measured data in MEMS spectrometer [12].

measurement data, while the blue and purple waveforms are control signals. The yellow output signal is a periodically repeating sequence of rectangular pulses. Each pulse represents a different spectral measurement interval about 10-nm-wide. These pulses cover the visible measurement range from 340 to 780 nm wavelength, so the girth of the yellow waveform corresponds to the

measured spectral distribution of the source in the visible range. The amplitude of a particular pulse corresponds to the flux value in its spectral measurement interval. Because the sensor can measure fluxes from a few pW to single μW, it must cooperate with a tunable pulse amplifier. Such an amplifier should guarantee the same frequency bandwidth for all gain levels. This condition cannot be met by the amplifier, which works according to the same principle as the circuit shown in Fig. 2. Therefore, a new amplifier solution was developed, which is described in the next part of this paper.

The principle of the new solution (Fig. 4) is connecting a multi-output cluster (ripple-curry) amplifier with a multi-input analog-to-digital converter. The proposed amplifier consists of M identical sections, for example, with 4, with 8 or 16 component amplifiers. The output of the previous section connects to the input of the next section and at the same time puts the signal into one of the converter's inputs. It is important to have similar frequency characteristics in all sections. Also important is the careful selection of gain values in each section.

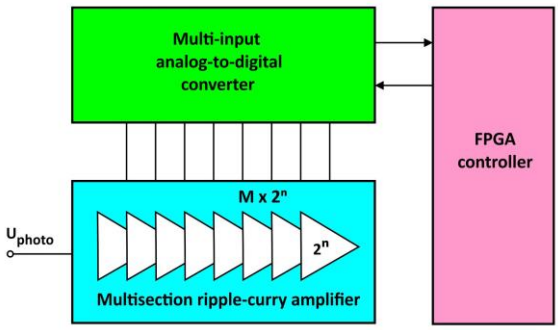

Fig. 4. Idea of the new measurement system.

Preferably if the gain of each section is a multiple of 2^n, that is, 2, 4, 8 and so on. Which makes it easier to backscale the converter's output signal, since dividing digital data in an FPGA by 2, 4 or 8 involves discarding the 1, 2 or 3 youngest bits.

This linking of circuit components allows to perform the automatic gain control function in a digital way. This is implemented by the FPGA chip, which periodically reads the amplitudes of the pulses on the subsequent inputs of the analogue-to-digital converter. And then selects the signal from one of the inputs where this signal is the largest, but it does not exceed the input range of the converter. Because the FPGA knows the inputs of the converter with the optimal signal, so it also knows how many times the signal from the MEMS spectrometer was amplified. Hence, to calculate the actual flux value (pulse amplitude) in a given spectral interval, it is enough to divide the digital data by the gain value, which can mean a right shift of n bits. In the system described, gain control is carried out in a natural clean electronic way. There are no mechanical switches or electronic keys that modify the frequency characteristics of the system. An example of the ripple-curry amplifier architecture that was investigated in the work is shown in Fig. 5.

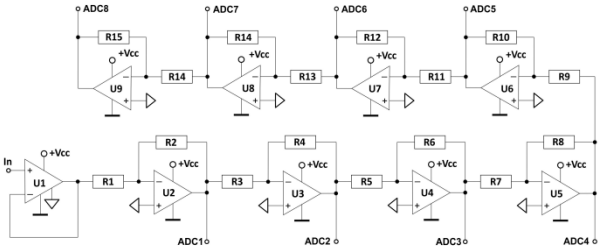

Fig. 5. Schematic of the tested ripple-curry amplifier.

This is a simplified version of the circuit, which only used to confirm the concept of a ripple-carry amplifier for a MEMS sensor. The frequency bandwidth of the individual sections is determined by the gain-bandwidth product of the single operational amplifier [13]. The incidental frequency bandwidth will be slightly narrower than the frequency bands of operational amplifiers. The analogue ground voltage in the circuit is equal to half the supply voltage Vcc. This voltage is automatically produced by the unit-gain input module U1 [14]. Each amplifier section had its resistance values chosen to give a gain of –2 V/V. Careful selection of resistance values is important for the symmetry of the entire circuit. Therefore, photoelectric pulses are amplified at the outputs of successive stages twice, by four times, by eight times, up to 256 times. If the single section gain was 4 in the above circuit, then the gain of the whole path could be more than 65000 times, or nearly 100 dB.

The particular sections of the described amplifier were built in the simplest way, that is, in the inverting amplifier circuit. Of course, such a circuit inverts the phase of the amplified signal. However, this is not a critical disadvantage, because the analog-to-digital converter can measure both low and high levels of the photoelectric pulse, and then the FPGA chip can calculate the pulse amplitude. The usage of inverting amplifiers has the added advantage of reducing the DC component accumulation at the outputs by inverting the pulse phase.

The final section of the paper shows the measured signal waveforms of the system for two different input signal frequencies. In the first case (Fig. 6), the photoelectric pulses were of low frequency, which was 5 kHz. In this case, the yellow input signal, whose amplitude was about 100 mV, is amplified twice by the first section of U2, which shows the blue signal at its output. The blue signal is then amplified by the U3 section, producing a purple signal that is inverted in phase and amplified another two times. This signal is amplified by U4 and transformed into a green signal at its output.

As confirmed by the included waveforms, the tested circuit does not distort the amplified pulse signals, which means that it can handle the MEMS spectrometer in this frequency range.

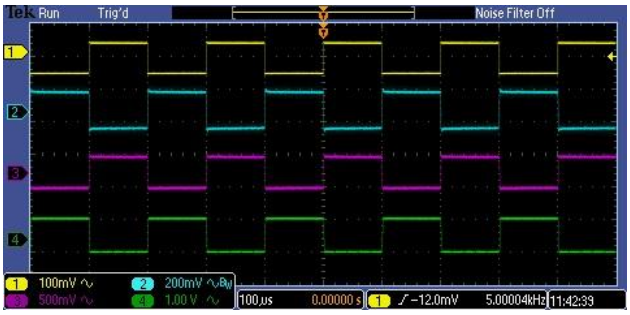

Fig. 6. Result 1: 5 kHz pulse amplification.

The tested circuit shows slightly less advantageous characteristics at higher frequencies, as shown in Fig. 7. Visible pulse distortion is a result of the frequency and timing parameters of the operational amplifiers used in the design. As can be seen in the figure, the amplitudes of the pulses are still measurable, but oscillations have appeared, and the slope of the pulses has decreased. The first effect comes from the missing frequency compensation in the amplification sections and from the too low frequency bandwidth of the operational amplifiers, since the used amplifiers have had the gain bandwidth product about 10 MHz. In contrast, the pulse slope depends on the slew rate parameter, which in the tested amplifiers was only 7 V/µs.

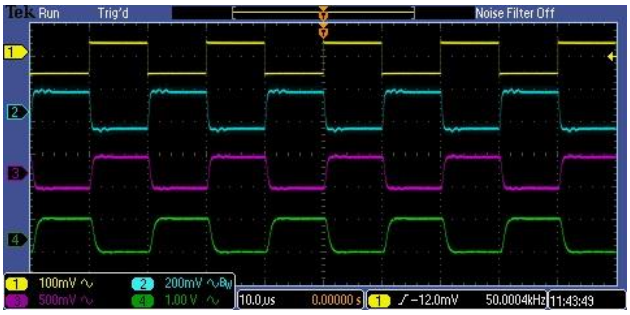

Fig. 7. Result 2: 50 kHz pulse amplification.

In summary, the aim of this paper was the presentation of the original chain amplifier circuit for conditioning the output signal from the optical MEMS sensor. Such an amplifier should not degrade the measurement performance of the whole system. Since the output signal is the amplitude-modulated pulse sequence, their amplifier should be wideband and containing the automatic gain control mechanism. The developed system and its measurements showed that such application may not be very complicated. In addition, the method of amplifying photoelectric pulses presented in the paper significantly simplifies data processing in a digital system.

References

[1] C. Ortolani, *Flow Cytometry Today. Detectors and Electronics*, (Springer 2022). pp. 97–119, [Online]. Available: https://link.springer.com/chapter/10.1007/978-3-031-10836-5_7, [Accessed: 20 Dec. 2022].

[2] D. Maes, L. Reis, S. Poelman, E. Vissers, V. Avramovic, M. Zaknoune, G. Roelkens, S. Lemey, E. Peytavit, B. Kuyken, *High-Speed Photodiodes on Silicon Nitride with a Bandwidth beyond 100 GHz*, Conference on Lasers and Electro-Optics, Optica Publishing Group, (2022), [Online]. Available: https://opg.optica.org/abstract.cfm?uri= cleo_si-2022-SM3K.3, [Accessed: 20 Dec. 2022].

[3] R. Das, Y. Xie, A.P. Knights, *All-Silicon Low Noise Photonic Frontend For LIDAR Applications*, 2022 IEEE Photonics Conference (IPC), IEEE Xplore (2022), [Online]. Available: https://ieeexplore.ieee.org/ abstract/document/99757507, [Accessed: 20 Dec. 2022].

[4] FEMTO Messtechnik GmbH, *Variable Gain Photoreceiver - Fast Optical Power Meter Series OE-200*, [Online]. Available: https://www.femto.de/en/products/photoreceivers/variable-gain-up-to-500-khz-oe-200.html, [Accessed: 20 Dec. 2022].

[5] M. Nehir, C. Frank, S. Aßmann, E.P. Achterberg, Sensors **19**(12), 2833 (2019). https://doi.org/10.3390/s19122833.

[6] F. Thomas,; R. Petzold, C. Becker, U. Werban, Sensors **21**(11), 3927 (2021). https://doi.org/10.3390/s21113927.

[7] M. Muhiyudin, D. Hutson, D. Gibson, E. Waddell, S. Song, S. Ahmadzadeh, Sensors **20**(14), 3843 (2020). https://doi.org/10.3390/ s20143843.

[8] S. Maruyama, T Hizawa, K. Takahashi, K. Sawada, Sensors **18**(1), 138 (2018). https://doi.org/10.3390/s18010138.

[9] S. Merlo, P. Poma, E. Crisà, D. Faralli, M. Soldo, Sensors **17**(3), 8 (2017). https://doi.org/10.3390/ s17030462.

[10] M.S. Wei, F. Xing, B. Li, Z. You, Sensors **11**(10), 9764 (2011). https://doi.org/10.3390/s111009764.

[11] Z. Yang, T. Albrow-Owen, W. Cai, T. Hasan, Science **371**, 6528 (2021). https://doi.org/ 10.1126/science.abe0722.

[12] Hamamatsu Photonics K.K. *Fingertip size, ultra-compact spectrometer head integrating MEMS and image sensor technologies*. [Online]. Available: https://www.hamamatsu.com/content/dam/hamamatsu-photonics/sites/documents/99_SALES_LIBRARY/ ssd/ c12666ma_ kacc1216e.pdf. [Accessed: 10 Dec. 2022].

[13] Microchip Technology Inc, *MCP6291/1R/2/3/4/5 1.0 mA 10 MHz Rail-to-Rail Op Amp*, [Online]. Available: https://ww1.microchip.com/ downloads/en/DeviceDoc/MCP6291-Family-Data-Sheet-DS20001812G.pdf. [Accessed: 10 Dec. 2022].

[14] Microchip Technology Inc. *MCP6021/1R/2/3/4 Rail-to-Rail Input/Output 10 MHz Op Amps*, [Online]. Available: https://ww1. microchip.com/downloads/aemDocuments/documents/APID/ProductDocuments/DataSheets/20001685E.pdf . [Accessed: 10 Dec. 2022].

